Available online at www.sciencedirect.com
SCIENCE DIRECT®

PERGAMON

Polyhedron 22 (2003) 1673–1682

POLYHEDRON

www.elsevier.com/locate/poly

# The adsorption of 2,2′:6′,2″-terpyridine, 4′-(5-mercaptopentyl)-2,2′:6′,2″-terpyridinyl, and perchlorate on silver and copper surfaces monitored by SERS

A.C. Sant'Ana [a], W.A. Alves [a], R.H.A. Santos [b], A.M.D. Ferreira [a], Marcia L.A. Temperini [a,*]

[a] *Departamento de Química Fundamental, Instituto de Química, Universidade de São Paulo, CEP 05513-970 Sao Paulo, SP, Brazil*
[b] *Instituto de Química de São Carlos, Universidade de São Paulo, CEP 13560-970 Sao Carlos, SP, Brazil*

Received 14 November 2002; accepted 15 April 2003

## Abstract

The adsorption of 2,2′:6′,2″-terpyridine on Ag and Cu electrode surfaces has been studied by using surface enhanced Raman spectroscopy (SERS). Two types of surface complexes have been found on a silver electrode: the first one is stable near the open circuit potential, having bonding between tpy and silver active site analogous to the Ag–N bonding in the $[Ag^I(tpy)Cl]\cdot 2H_2O$ complex; and the second one is stable in the −0.1 to −0.5 V (Ag/AgCl) potential range, where the interaction between tpy and silver active site is similar to the Cu–N bonding in the $[Cu^{II}(tpy)Cl_2]$ complex. The SERS spectra of 4′-(5-mercaptopentyl)-2,2′:6′,2″-terpyridinyl (tpy–SH) have shown an increase in the relative intensity of the mercaptopentyl moiety bands and a band at 310 $cm^{-1}$, assigned to the AgS stretching, indicating an adsorption through the S atom. In addition, using the Raman results of different copper perchlorate salts obtained with different hydration degrees, it has been possible to characterize the adsorption of perchlorate anion on silver electrode and the kind of coordination in the $[Cu^{II}(tpy)(H_2O)(ClO_4)]ClO_4$ and $[Cu^{II}(tpy)(H_2O)(ClO_4)_2]$ complexes.

*Keywords:* SERS; Terpyridine; Perchlorate

## 1. Introduction

Amine and thiol compounds are easily adsorbed on metallic surfaces, allowing for the preparation of chemically modified electrodes, molecular devices and sensors, where they can be used as supports for other adsorbates [1,2]. These systems are particularly suitable for surface enhanced Raman spectroscopy (SERS) investigations, which is excellent tool for analyzing adsorbate metal chemical interactions [3,4]. The adsorption behavior of cyclic amines, such as 2,2′-bipyridine and imidazole, has been studied by SERS [5–8] and the formation of surface complexes has been proposed [9–11]. Particularly, the 2,2′:6′,2″-terpyridine (tpy) and substituted tpy are useful as building blocks for supramolecular coordination oligomers, due to their strong ligand character [12]. Some of its transition metal complexes exhibit photophysical properties [13–16] that lead to interesting molecular devices [17–20].

Maskus and Abruña have synthesized and characterized the 4′-(5-mercaptopentyl)-2,2′:6′,2″-terpyridinyl (tpy–SH). They have used it to obtain surface immobilized complexes of $Co^{II}$ and $Os^{II}$, since the tpy–SH surface adsorption has occurred through the sulfur atom, and the coordination of the metal ions is through the nitrogen atoms of tpy moiety. These systems have exhibited electrocatalytic behavior towards the reduction of nitric oxide [21].

In this work, the adsorptions of tpy and tpy–SH on metal surfaces from different mother-solutions have

---

* Corresponding author. Tel.: +55-11-3091-3853; fax: +55-11-3091-3890.
*E-mail address:* mlatempe@quim.iq.usp.br (M.L.A. Temperini).

0277-5387/03/$ - see front matter © 2003 Elsevier Science Ltd. All rights reserved.
doi:10.1016/S0277-5387(03)00325-5

been monitored by SERS for the first time, aiming at characterizing the nature of the adsorbed species. Additionally, the characterization of $ClO_4^-$ ion, adsorbed on a metallic surface and coordinated in the corresponding $Cu^{II}$–tpy complexes, has been presented.

## 2. Experimental

### 2.1. Materials

Terpyridine (tpy) from Aldrich Chemical Co. has been purified by sublimation under vacuum to obtain the Raman spectrum and used without further purification in the SERS experiments. The tpy–SH has been kindly donated by Prof. Hector D. Abruña. Deionized water and p.a. grade chemicals have been used for all prepared solutions. The anhydrous $Cu(ClO_4)_2$ salt has been obtained by heating the hexahydrate salt under vaccum, at about 100 °C, as described by Hathaway and Underhill [22].

### 2.2. Synthesis of Cu–tpy and Ag–tpy complexes

#### 2.2.1. $[Cu^{II}(tpy)(H_2O)(ClO_4)]ClO_4$

To a solution of tpy (119 mg, 0.5 mmol) in methanol (20 $cm^3$), a solution of $Cu(ClO_4)_2 \cdot 6H_2O$ (189 mg, 0.5 mmol) dissolved in methanol (10 ml) has all at once been added under stirring at room temperature. The solution has turned from blue to greenish during the reaction. The solution was kept in a freezer for 3 days, yielding a microcrystalline precipitate, which was collected by filtration, washed with cooled diethyl ether, and then dried in vacuum. Yield: 77%. *Anal.* Found: C, 35.29; H, 2.46; N, 8.22. Calc. for $[CuN_3C_{15}OH_{13}(ClO_4)] \cdot (ClO_4)$: C, 35.07; H, 2.55; N, 8.18%. $\Lambda_M = 131$ S $cm^2$ $mol^{-1}$ in water. UV–Vis (methanol, $\lambda_{max}$, nm ($\varepsilon$, $M^{-1}$ $cm^{-1}$)): 222 (24250), 266 (14050), 275 (14750), 283 (14700), 325 (13950), 338 (13750), 693 (65). EPR: $g_\perp$, 2.067; $g_\parallel$, 2.277; $A_\parallel$ ($10^{-4}$ $cm^{-1}$), 178; $g_\parallel/A_\parallel$ (cm), 128 in frozen methanol/water (4:1, v/v) solution at 77 K.

#### 2.2.2. $[Cu^{II}(tpy)(H_2O)(ClO_4)_2]$

This mononuclear complex has been obtained through slow evaporation of the above-mentioned complex solution at room temperature. In this case, crystals suitable for X-ray data collection have been obtained.

#### 2.2.3. $[Cu^{II}(tpy)Cl]Cl$ and $[Ag^{I}(tpy)Cl] \cdot 2H_2O$

These complexes have been obtained through a procedure similar to the one described above, except for the addition of a solution of $CuCl_2 \cdot 2H_2O$ or $AgNO_3$ dissolved in methanol. $[Cu^{II}(tpy)Cl]Cl$: Yield: 83%. *Anal.* Found: C, 48.88; H, 3.07; N, 11.17. Calc. for $[CuN_3C_{15}H_{11}Cl_2]$: C, 49.00; H, 3.01; N, 11.43%. $\Lambda_M = 113$ S $cm^2$ $mol^{-1}$ in water. UV–Vis (methanol, $\lambda_{max}$, nm ($\varepsilon$, $M^{-1}$ $cm^{-1}$)): 222 (66800), 263 (31933), 275 (24600), 285 (22533), 325 (25466), 340 (26133), 705 (204). EPR: $g_\perp$, 2.063; $g_\parallel$, 2.250; $A_\parallel$ ($10^{-4}$ $cm^{-1}$), 174; $g_\parallel/A_\parallel$ (cm), 129 in frozen methanol/water (4:1, v/v) solution at 77 K. $[Ag^{I}(tpy)Cl] \cdot 2H_2O$: Yield: 75%. *Anal.* Found: C, 42.92; H, 2.95; N, 9.80. Calc. for $[AgN_3C_{15}H_{15}O_2Cl]$: C, 43.60; H, 3.60; N, 10.20%.

### 2.3. Structure determination of $[Cu^{II}(tpy)(H_2O)(ClO_4)_2]$

A single crystal of $[Cu^{II}(tpy)(H_2O)(ClO_4)_2]$ has been mounted on an Enraf-Nonius turbo CAD4 diffractometer at room temperature, by using 25 ($\theta$ from 11.66 to 18.25°) automatically centered reflections, and the cell parameters have been obtained and refined. Table 1 shows the data collection and the refinement conditions. The data have been corrected for absorption ($\mu$(Mo K$\alpha$) = 1.495 $mm^{-1}$) by using the PSISCAN method [23]. The structure has been solved by using the WinGX system [24] by SIR-92 [25], and refined by full-matrix least-squares and difference Fourier synthesis [26]. The hydrogen atoms have been placed in their ideal positions, except for the non-refined water molecule. The thermal displacement for the hydrogen atoms has been set equal to 1.3 times the isotropic equivalent B of the attached atom. All non-hydrogen atoms have been

Table 1
Crystal data and details of the structure determination for $[Cu^{II}(tpy)(H_2O)(ClO_4)_2]$

| | |
|---|---|
| Formula | $C_{15}H_{13}Cl_2CuN_3O_9$ |
| Formula weight | 513.73 |
| Temperature (K) | 293 |
| Crystal system | orthorhombic |
| Space group | $Pna2_1$ |
| $a$ (Å) | 19.289(2) |
| $b$ (Å) | 8.5624(7) |
| $c$ (Å) | 11.4502(9) |
| $V$ (Å$^3$) | 1891.1(3) |
| $Z$ | 4 |
| $D_{calc}$ (Mg $m^{-3}$) | 1.804 |
| $\mu$(Mo K$\alpha$) ($mm^{-1}$) | 1.495 |
| $F$(0 0 0) | 1036 |
| Crystal size (mm) | 0.10 × 0.10 × 0.10 |
| Radiation (Å) Mo K$\alpha$ | 0.71073 |
| $\theta$ min., max. (°) | 2.6, 30.0 |
| Dataset | $\overline{12}$:0:16; $\overline{27}$:0 |
| Total, unique data | 3132, 2872 |
| Observed data [$I > 2.0\sigma(I)$] | 1626 |
| $N_{ref}$, $N_{par}$ | 2872, 280 |
| $R$, $wR_2$, $S$ | 0.0416, 0.1123, 1.00 |
| $w = 1/[\sigma^2(F_o^2)+(0.0514P)^2]$ | where $P = (F_o^2+2F_c^2)/3$ |
| Max. and average shift/error | 0.00, 0.00 |
| Flack $x$ | −0.02(2) |
| Min. and max. resd. dens. (e Å$^{-3}$) | −0.73, 0.47 |

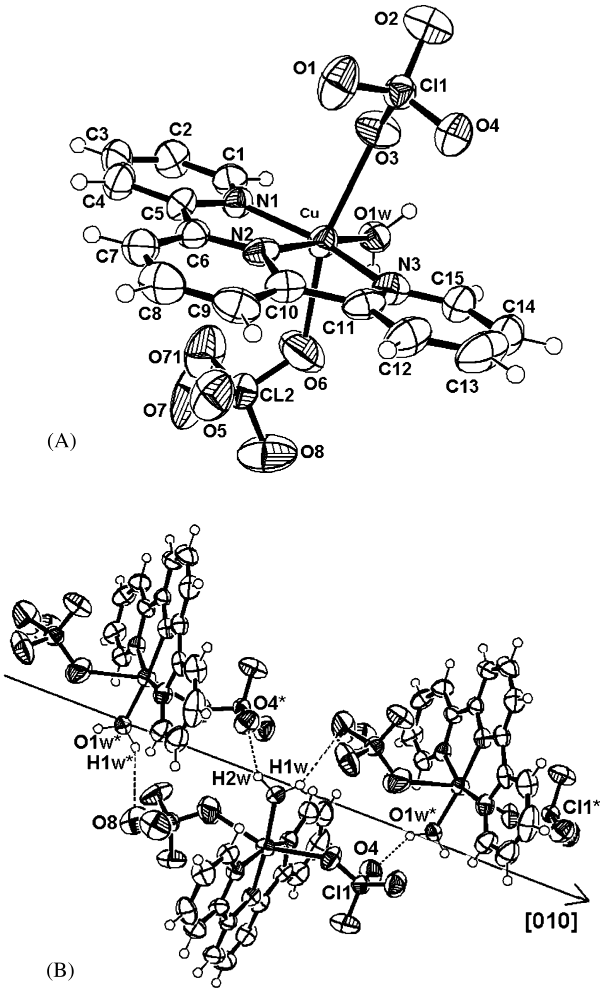

Fig. 1. ORTEP representation (50% of probability) for the [Cu$^{II}$(tpy)(H$_2$O)(ClO$_4$)$_2$] (a) asymmetric unit (b) polymeric chain.

refined anisotropically. The structural analysis has been performed by PLATON system [27].

In the [Cu$^{II}$(tpy)(H$_2$O)(ClO$_4$)$_2$] asymmetric unit (Fig. 1(a)), the Cu atom has a coordination number equal to 6 in a distorted octahedral arrangement, with two ClO$_4^-$ ions in apical positions and the tpy and water molecules in equatorial positions. The supramolecular crystal structure (Fig. 1(b)) consists of a polymeric chain of [Cu$^{II}$(tpy)(H$_2$O)(ClO$_4$)$_2$] units, linked by hydrogen bonds. The selected bond distances and angles are shown in Table 2, which includes the hydrogen bonds.

Table 2
Bond distances (Å) and angles (°) for [Cu$^{II}$(tpy)(H$_2$O)(ClO$_4$)$_2$]

| | | | | |
|---|---|---|---|---|
| *Bond distances* | | | | |
| Cu–O1w | 1.952(4) | Cu–O3 | 2.440(5) | |
| Cu–O6 | 2.450(8) | Cu–N1 | 2.025(5) | |
| Cu–N2 | 1.922(4) | Cu–N3 | 2.013(5) | |
| Cl1–O1 | 1.418(4) | Cl2–O5 | 1.428(6) | |
| Cl1–O2 | 1.428(6) | Cl2–O6 | 1.433(8) | |
| Cl1–O3 | 1.433(5) | Cl2–O8 | 1.412(7) | |
| Cl1–O4 | 1.436(5) | Cl2–O71 [a] | 1.423(17) | |
| | | Cl2–O7 [a] | 1.43(2) | |
| O1w–H2w | 0.8798 | O1w–H1w | 0.9000 | |
| *Bond angles* | | | | |
| O1w–Cu–O3 | 79.5(2) | O1w–Cu–O6 | 78.6(2) | |
| O1w–Cu–N1 | 97.0(2) | O1w–Cu–N2 | 175.4(2) | |
| O1w–Cu–N3 | 101.7(2) | O3–Cu–O6 | 157.7(2) | |
| O3–Cu–N1 | 94.0(2) | O3–Cu–N2 | 104.6(2) | |
| O3–Cu–N3 | 91.9(2) | O6–Cu–N1 | 93.1(2) | |
| O6–Cu–N2 | 97.5(2) | O6–Cu–N3 | 88.2(2) | |
| N1–Cu–N2 | 80.6(2) | N1–Cu–N3 | 161.1(2) | |
| N2–Cu–N3 | 80.5(2) | H1w–O1w–H2w | 113.6 | |
| Cu–O1w–H1w | 126.27 | Cu–O1w–H2w | 116.8 | |
| A–B–C | dB···C (Å) | dA···C (Å) | Angle (°) | Symmetry |
| O1w–Hw–O8 | 1.800 | 2.689(8) | 169.0 | $-x, -1/2+y, -z$ |
| O1w–H2w–O4 | 2.018 | 2.800(7) | 147.6 | $-x, 1/2+y, -z$ |

[a] Disordered oxygen atom (occupation factor = 0.5).

## 2.4. SERS procedure

For SERS and electrochemical experiments, the working electrode was a polycrystalline Ag (99.99%) or Cu (99.9%) rod into a Teflon holder, with an exposed surface of 10 mm$^2$. The counter and reference electrode were Pt wire and Ag/AgCl, respectively. The metallic surface of the working electrode has been pre-treated by mechanical polishing with emery paper of 1000 mesh.

The SERS activation of the electrode has been done by oxidation–reduction cycles (ORC) with 1 mA oxidation peak currents, using $10^{-1}$ mol l$^{-1}$ electrolyte salt aqueous solution. In all of the SERS experiments, the ORC procedures have been carried out in electrolyte solution without the presence of the sample. The anions and solvent used in the activation procedures were the same used in the SERS experiments.

For the ex situ SERS experiments after the activation, the electrode was copiously washed and dipped into a mother-solution containing $10^{-3}$ mol l$^{-1}$ of the sample. After 1 h of self-assembly, the SERS spectra were obtained. For acidic solutions, the desired pH has been achieved by using HCl, HClO$_4$ or HI, depending on the kind of the anions used in the mother-solutions. The chosen pH value was 1.8, below the tpy second p$K_a$ value (p$K_a$ = 3.0) [28,29].

For the in situ SERS experiments after the activation procedure, the cell and the electrode were copiously washed and a new solution was used containing $10^{-3}$ mol l$^{-1}$ of the same electrolyte salt and sample. After 1 h at the open circuit condition, the SERS spectra were obtained.

### 2.5. Instrumentation

Raman excitation has been provided by the 632.8 nm line of a Spectra Physic He–Ne laser, model 127, using a Renishaw spectrometer, model System 3000, with Olympus BTH-2 microscopy with 50 × objective lens and Charge Coupled Device (CCD) Detector. The infrared spectra were taken on a KBr pellet made with the compounds, recorded with a FTIR Bomem model BM-100, with KBr beam-splitter and DTGS detector, at 4 $cm^{-1}$ resolution. Electrochemical experiments have been carried out in an EG&G potentiostat–galvanostat, model Princeton Applied Research (PAR) 263.

## 3. Results and discussion

In the ex situ SERS experiments, adsorbate species have been characterized as a function of the nature of the mother-solution. The SERS spectra obtained are shown in Fig. 2. The role of applied potentials, the electrolytic solutions and the kind of metallic surfaces on the nature of the adsorbed species have also been investigated by in situ SERS experiments. These SERS spectra are shown in Fig. 3. The Raman spectra of standard compounds with tpy in different chemical environments (shown in Fig. 4) have been used as references to identify the chemical interactions of adsorbate with the electrode surface. The frequency values and the assignment for tpy [30], Me–N and $ClO_4^-$ modes are shown in Table 3.

The ex situ SERS spectra of tpy–SH adsorbed on Ag surfaces from mother-solutions of different anions, with and without $Cu^{II}$ ions, have been obtained and are shown in Fig. 5. These results have confirmed the proposed adsorption behavior of tpy based on SERS spectra.

Based on Raman studies of copper perchlorate salts with different degrees of hydration (Fig. 6 and Table 4), the adsorption type of $ClO_4^-$ electrolytic anions on the Ag surface, and its different coordination states in $Cu^{II}$–tpy–$ClO_4^-$ complexes, have been analyzed (Fig. 7).

### 3.1. Ex situ SERS experiments

The ex situ SERS spectra of tpy adsorbed on Ag electrodes, activated by ORC in $Cl^-$ electrolyte solution, have shown the same species on the surface, independently from the mother-solutions pH (Fig. 2(a and b)). These results have indicated that the $tpyH_2^{2+}$ species, which is mostly present at pH 1.8, suffers deprotonation when adsorbed on the electrode surface. The SERS spectrum of the adsorbed species is characterized by the bands at 721, 1005, 1319, 1564 and 1588 $cm^{-1}$, and its pattern is very similar to that of the $[Ag^I(tpy)Cl]\cdot 2H_2O$ complex (Fig. 4(c)). This result has indicated that a surface complex involving tpy and Ag adatom is formed and that this species has a bonding

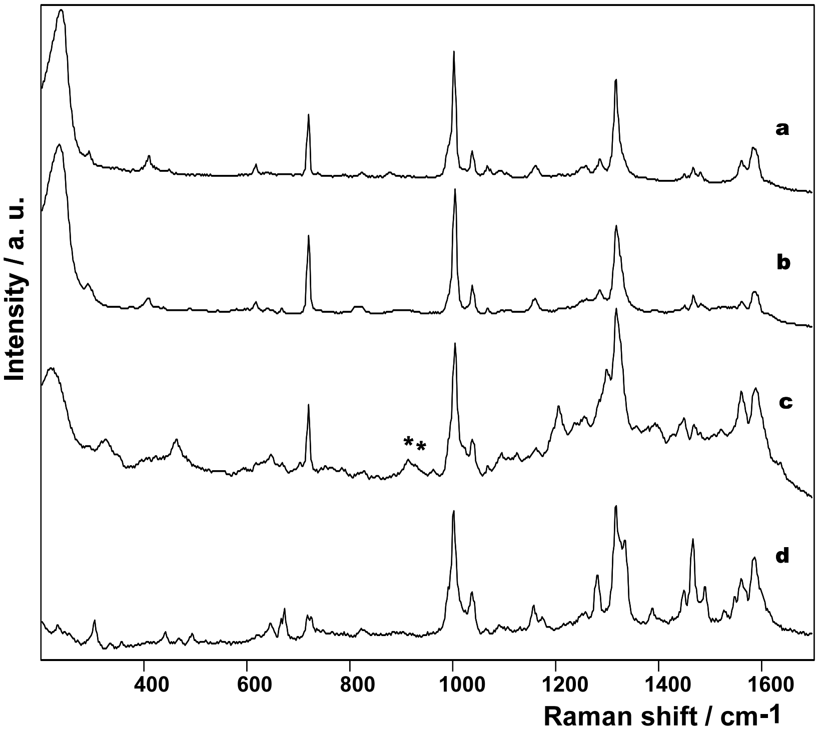

Fig. 2. Ex situ SERS spectra of tpy adsorbed on Ag electrode surface obtained from the following mother-solutions: $Cl^-$, ethanol (a), $Cl^-$, water, pH 1.8 (b), $ClO_4^-$, water (c) $I^-$, water, pH 1.8 (d). * Raman bands of perchlorate adsorbate.

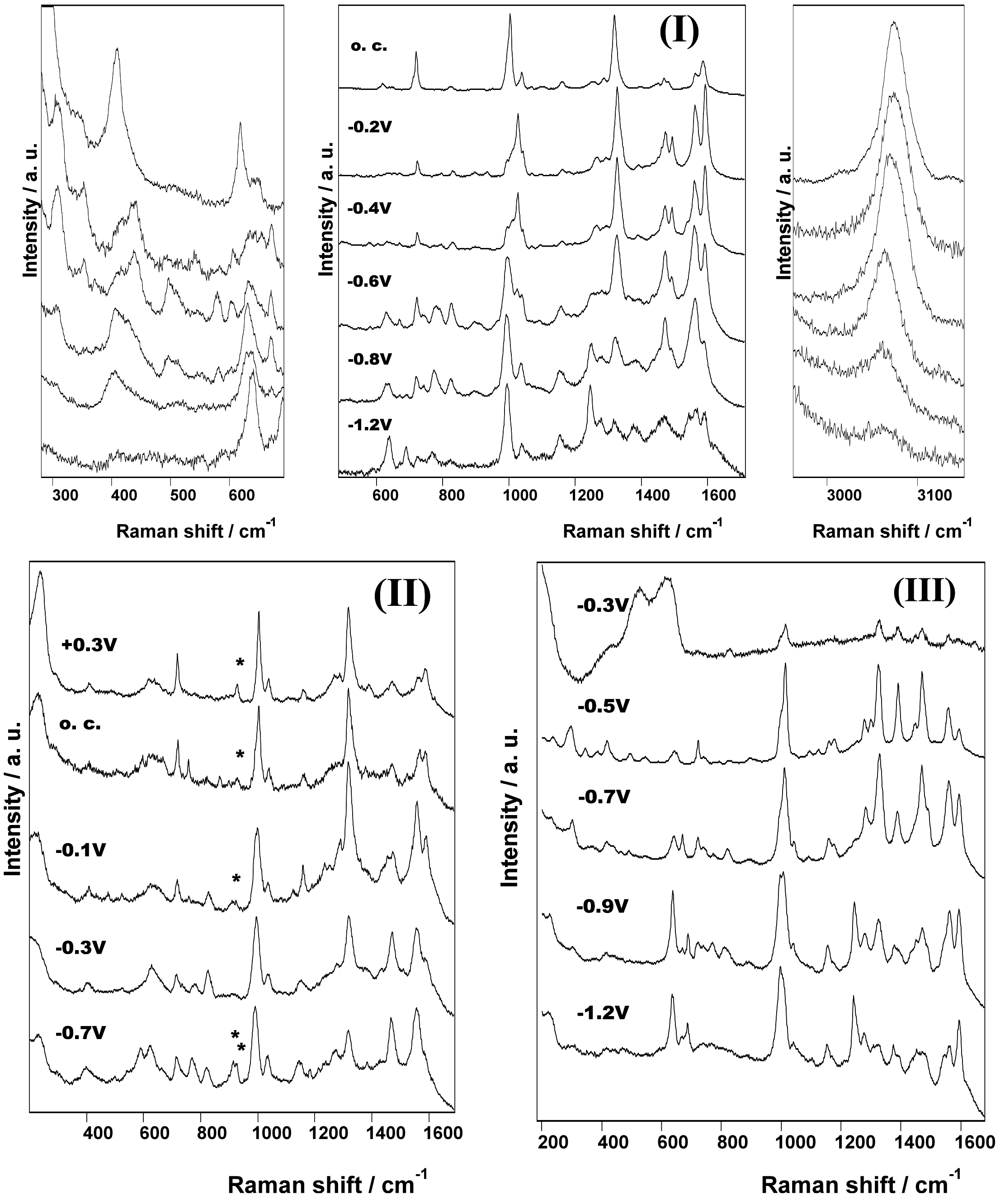

Fig. 3. In situ SERS spectra of the systems: (**I**) Ag/tpy(aq.)/$Cl^-$; (**II**) Ag/tpy(aq.)/$ClO_4^-$; (**III**) Cu/tpy(aq.)/$Cl^-$. * Raman bands of perchlorate adsorbate.

structure similar to that of the synthesized complex. In both complexes, the tpy molecules are coordinated by the lone electron pair of nitrogen atoms. This can be verified when the band assigned to the symmetric ring breathing mode shifts up from 995 $cm^{-1}$ (free tpy) to 1005 $cm^{-1}$.

The same kind of surface complex has been formed on Ag electrode, when it is activated in a $ClO_4^-$ electrolyte solution (Fig. 2(c)). The presence of $ClO_4^-$ on the surface is confirmed by the bands at 916 and 930 $cm^{-1}$. The broadening of the tpy bands and the decrease in the signal/noise ratio of the spectrum have suggested that the silver adatoms are not stabilized by perchlorate anions and, therefore, different types of interactions with tpy exist. When $I^-$ ions are adsorbed on the electrode surface (Fig. 2(d)), the SERS spectrum is different, and new bands typical of $tpyH_2^{2+}$ are observed at 1015 (sh), 1335 and 1615 (sh) $cm^{-1}$ (Fig. 4(b)). In this case, although the tpy is the predominant adsorbed species, the protonated species have also been detected, due to the formation of an ion-pair with the $I^-$ adsorbed.

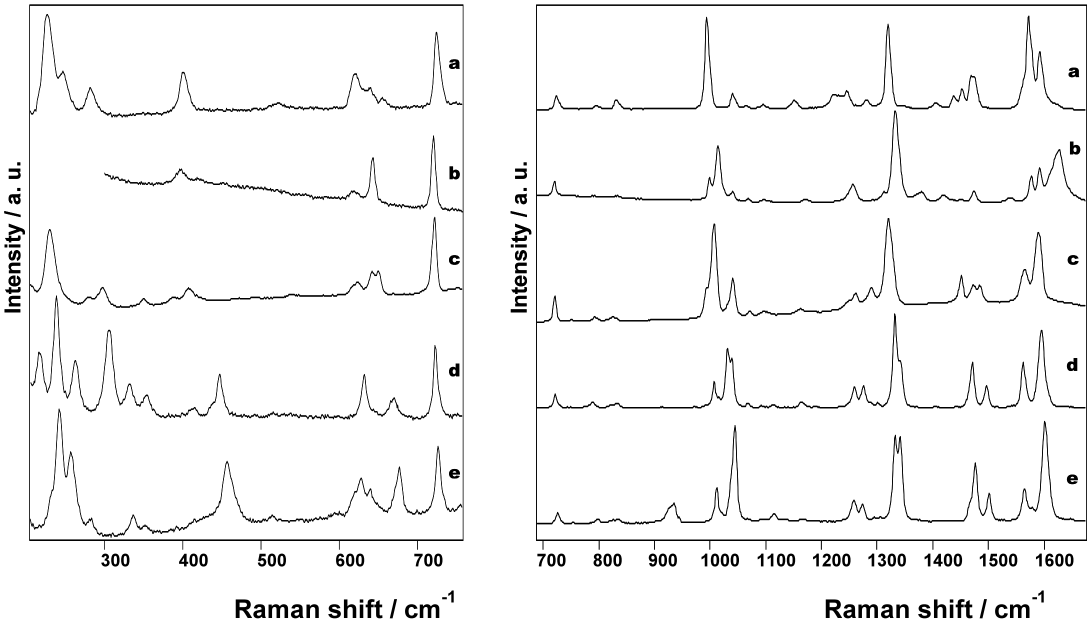

Fig. 4. Normal Raman spectra of the standard compounds: tpy solid (a), tpy$H_2^{2+}$(aq.) (b), [$Ag^I$(tpy)Cl]·2$H_2O$ solid (c), [$Cu^{II}$(tpy)$Cl_2$] solid (d), [$Cu^{II}$(tpy)($H_2O$)($ClO_4$)]$ClO_4$ solid, same spectrum of Fig. 7(b) (e).

### 3.2. *In situ SERS experiments*

The in situ SERS spectrum of tpy adsorbed on Ag electrode in 0.1 mol l$^{-1}$ KCl aqueous solution (Fig. 3(**I**)), at open circuit potential, is similar to the ex situ spectra, and the stable adsorbed species are the same surface complex, called type I complex. By changing the potential to more negative values (−0.1 and −0.2 V), new interactions between tpy and Ag active sites appear, causing a novel spectral pattern characterized by the bands at 724, 1027, 1328, 1473, 1493, 1563 and 1593 cm$^{-1}$. This spectrum is similar to the spectra of the $Cu^{II}$–tpy complexes (Fig. 4(d and e)) and this surface complex has been called type II. The greater shifting up of the bands due to the symmetric ring breathing, the CC inter-ring and CC ring stretching modes from 1005, 1319 and 1588 cm$^{-1}$ to 1027, 1328 and 1593 cm$^{-1}$, respectively, suggest that in this kind of complex there is a strong bonding between the lone electron pair of the nitrogen atoms and the Ag active sites. During the cathodic sweep, the band of symmetric ring breathing at 1027 cm$^{-1}$ shifts down to 994 cm$^{-1}$, and the band at 350 cm$^{-1}$, assigned to the Ag–N stretching and observed in the standard spectrum of Ag–tpy complex (Fig. 4(c)), disappears. Simultaneously, there is a decrease in the relative intensity of the bands due to the C–H stretching. All these spectral features are consistent with a change from a perpendicular to a flat position in the orientation of tpy on the surface, and the spectrum at −1.2 V corresponds to the tpy physisorbed on the electrode surface.

When $ClO_4^-$ is the electrolyte anion (Fig. 3(**II**)), the surface complex type I is formed on the metallic surface at open circuit and more positive potential. Although it is not the predominant species on the electrode, the surface complex type II forms when the potential is scanned from 0.0 to −0.1 V. Its presence is confirmed by the decrease in the relative intensity of the band at 721 cm$^{-1}$, the appearance of the bands at 1015 and 1333 cm$^{-1}$, and the increase in the relative intensities of the bands at 1560 and 1593 cm$^{-1}$. At more negative potentials (−0.7 V), flat adsorption of the tpy on the metallic surface is favored, as already observed in the Ag/tpy/$Cl^-$ system. The adsorption of $ClO_4^-$ anions on silver electrode will be discussed later.

The adsorption of the tpy on a silver electrode in the presence of $I^-$ anions is the same as the one observed in the Ag/tpy/$Cl^-$ system (spectra not shown).

The surface spectrum, at open circuit potential for the Cu/tpy system in 0.1 mol l$^{-1}$ KCl electrolyte solution, mainly exhibits the bands of copper oxide (spectrum not shown). However, when the applied potential is −0.5 V, the copper oxide suffers a reduction, and the surface complex type II is formed (Fig. 3(**III**)), characterized by the bands at 721, 1013, 1327, 1390, 1470, 1557 and 1594 cm$^{-1}$. In these SERS spectra, the bands observed at 345 and 385 cm$^{-1}$, which also appear in the spectra of Cu–tpy complexes (Fig. 4(e and f)), are assigned to Cu–N stretching mode. These bands disappear at more negative potential than −0.9 V, when the tpy is physisorbed.

### 3.3. *Tpy–SH ex situ SERS experiments*

By comparing the normal Raman spectrum of tpy–SH (Fig. 5(a)) to the SERS spectra of tpy–SH adsorbed on Ag electrodes, when $Cl^-$ or $I^-$ were the electrolyte

Table 3
Raman frequency values (in cm$^{-1}$) of standard compounds

| Tpy | $TpyH_2{}^{2+}$ | $[Ag^I(tpy)Cl]\cdot 2H_2O$ | $[Cu^{II}(tpy)Cl]Cl$ | $[Cu^{II}(tpy)(H_2O)(ClO_4)]ClO_4$ | Assignment |
|---|---|---|---|---|---|
| 227 | | 231 | 216 | 243 | $\phi$(CC) ($\chi$ sens.) |
| 245 | | 279 | 238 | 257 | $\phi$(CC) ($\chi$ sens.) |
| 283 | | 297 | 262 | 283 | $\alpha$(CCC) ($\chi$ sens.) |
| 401 | 397 | 408 | 447 | 457 (*) | $\phi$(CC) (* $\alpha$ OClO) |
| | | 350/389 | | | $\nu$(AgN) |
| | | | 332/354 | 337/351 | $\nu$(CuN) |
| | | | 305 | | $\nu$(CuCl) |
| 522 | | 538 | | 514 | $\alpha$(CCC) |
| 622 | 619 | 623 | 631 | 627 (*) | $\alpha$(CCC)/(* $\rho$ $ClO_4$) |
| 639 | | 641 | 641 | 640 | $\alpha$(CCC) ($\chi$ sens.) |
| 655 | 643 | 650 | 669 | 677 | $\alpha$(CCC) |
| 724 | 721 | 721 | 722 | 726 | $\alpha$(CCC) ($\chi$ sens.) |
| 796 | 790 | 793 | 790 | 798 | $\phi$(CC) ($\chi$ sens.) |
| 832 | 833 | 825 | 825/834 | 825/834 | $\phi$(CC) ($\chi$ sens.) |
| | | | | 932 | $\nu$($ClO_4$) |
| 994 | 1000/1015 | 995(sh)/1008 | 1008/1032 | 1013/1045 | $\nu$(CC, CN) (ring breath.) |
| 1041 | 1041 | 1041 | 1040 | 1040(sh) | $\beta$(CH)/$\nu$(CC, CN) |
| 1064 | 1069 | 1072 | 1068 | 1068 | $\beta$ (CH)/$\nu$(CC, CN) |
| 1096 | 1099 | 1097 | 1094 | 1095 | $\beta$(CH)/$\nu$ (CC, CN) |
| | | | | 1115 | $\alpha$(OClO) |
| 1152 | 1172 | 1164 | 1165 | 1165 | $\beta$(CH)/$\nu$(CC, CN) |
| 1224 | | 1251 | 1259 | 1259 | $\nu$(CC, CN)/(Kekulé) |
| 1246 | 1258 | 1262 | 1276 | 1275 | $\nu$(CC, CN)/$\beta$(CH) |
| 1281 | 1313 | 1291 | 1301 | 1305 | $\beta$(CH) |
| 1320/1325(sh) | 1334/1343 | 1321/1330 | 1333/1342 | 1333/1342 | $\nu$(CC) inter-ring |
| 1406 | 1380 | | | | $\nu$(CC, CN)/$\beta$(CH) |
| 1438 | 1421 | 1452 | 1462(sh) | 1496(sh) | $\nu$(CC, CN)/$\beta$(CH) |
| 1453 | 1453 | 1473 | 1472 | 1477 | $\nu$(CC, CN)/$\beta$(CH) |
| 1470 | 1475 | 1486 | 1498 | 1501 | $\nu$(CC, CN)/$\beta$(CH) |
| 1475 | | | | | Fermi resonance |
| 1563(sh)/1573 | 1578/1593 | 1566 | 1563 | 1565 | $\nu$(CC) |
| 1573/1593 | 1610(sh)/1628 | 1590 | 1596 | 1602 | $\nu$(CC) |
| 3016 | | | 3037 | | $\nu$(CH) |
| 3054(sh) | | 3050 | 3061 | | $\nu$(CH) |
| 3066 | | 3080 | 3073 | 3080 | $\nu$(CH) |
| 3090 | | | 3095 | 3100 | $\nu$(CH) |

*$ClO_4^-$ +tpy bands.

anions during the electrode activation procedure (Fig. 5(b and c)), it can be seen that there is an increase in the relative intensity of the bands assigned to the alkyl–thiol moiety: 1015 and 1025 cm$^{-1}$ assigned to aliphatic C–C stretching, 1282 cm$^{-1}$ assigned to $CH_2$ wagging, 653 cm$^{-1}$ assigned to C–S stretching gauche conformer, and 2870 and 2925 cm$^{-1}$ assigned to aliphatic C–H stretching [31,32]. These intensity enhancements, together with the presence of the band at 310 cm$^{-1}$ assigned to the Ag–S stretching [33], suggest that the alkyl–thiol moiety is closer to the surface than the tpy moiety, and confirm that the adsorption occurs through the thiolate group [21]. It is important to note that, for this kind of adsorption, the symmetric breathing mode of the rings is observed at 995 cm$^{-1}$, which is similar to the frequency value assigned to tpy flat adsorbed in in situ SERS experiments, at very negative potential values. This coincidence supports the analysis of tpy adsorption presented above.

The Ag/tpy–SH surface, when dipped into the $CuBr_2$ ethanolic mother-solution, presents the spectrum showed in Fig. 5(d). There are no changes in the relative intensity of the bands and only the band assigned to the symmetric ring breathing shifts up to 1015 cm$^{-1}$. This result indicates that the adsorption still occurs through the alkyl–thiol moiety, but the $Cu^{II}$ atoms are now fixed on to the surface through coordination with the tpy moiety.

### 3.4. *Adsorption of $ClO_4^-$ on SERS active sites and its coordination in $Cu^{II}$–tpy complexes*

To characterize the adsorption and complexation of the $ClO_4^-$ species on a silver electrode, and in the $Cu^{II}$–tpy complexes, the Raman spectra of $ClO_4^-$ ions in copper perchlorate salts, with different hydration degrees, have been obtained.

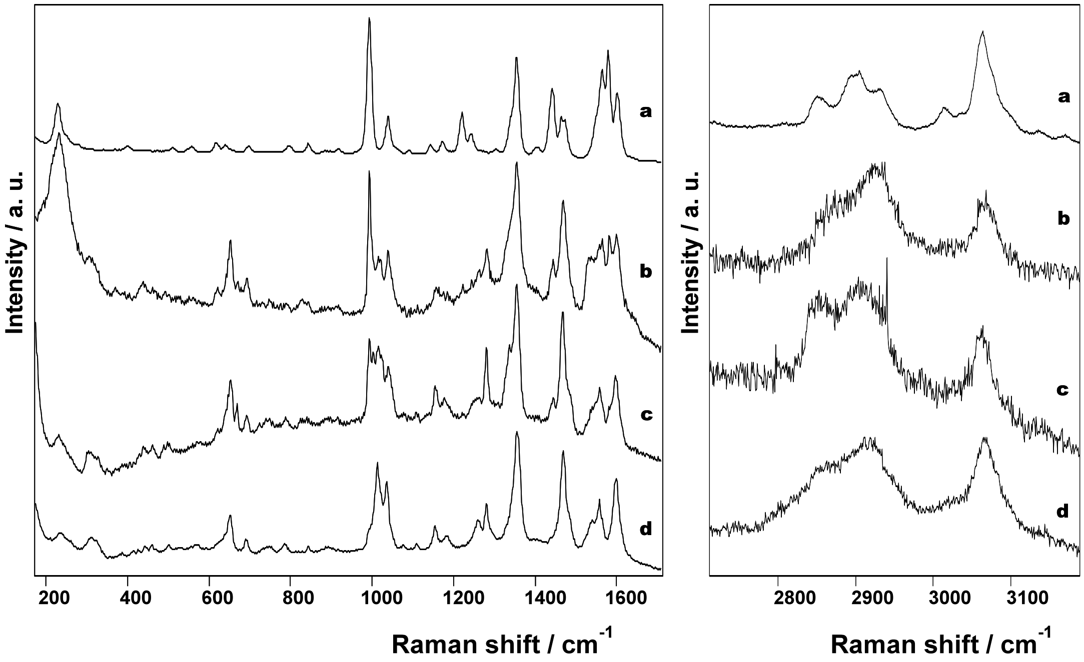

Fig. 5. Normal Raman spectrum of tpy–SH solid (a) and ex situ SERS spectra of: Ag/tpy–SH/Cl$^-$ (b), Ag/tpy–SH/I$^-$ (c), Ag/tpy–SH, Cu$^{2+}$/I$^-$, Br$^-$ (d). The tpy–SH self-assembled were obtained from ethanolic solutions.

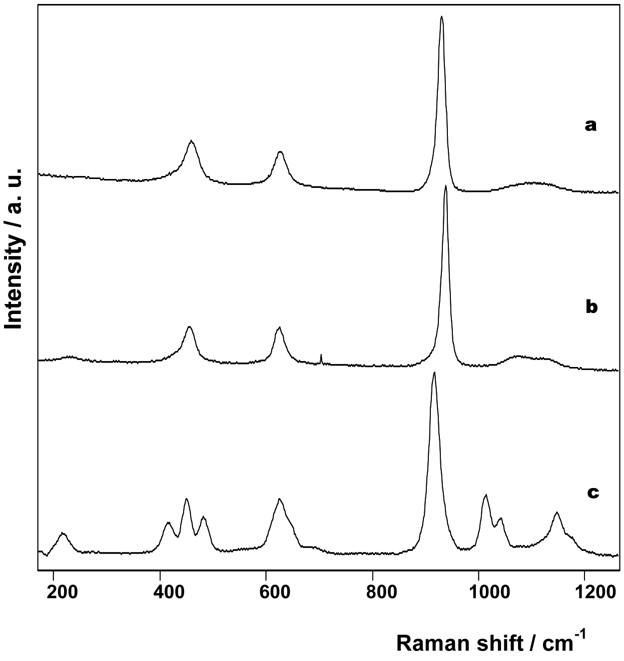

Fig. 6. Raman spectra of copper perchlorate solid: $[Cu^{II}(H_2O)_4](ClO_4)_2(H_2O)_2$ (a), $[Cu^{II}(H_2O)_2(ClO_4)_2]$ (b) and $[Cu^{II}(ClO_4)_2]$ (c).

The spectra of Fig. 6 have been obtained by heating of the $Cu(ClO_4)_2\cdot 6H_2O$, following the procedure described in Ref. [22]. As the degree of hydration decreases, the formation of Cu–perchlorate bonding occurs, and there is a simultaneous change in the $ClO_4$ symmetry from $T_d$ (non-coordinated) to $C_{3v}$ (monocoordinated), and then to $C_{2v}$ (bicoordinated). The shift of the band, due to the symmetric $ClO_4$ stretching mode, and the increase in the number of bands, due to the breakdown of the degeneracy of the bands assigned to the $E$ and $F_2$ modes, can be clearly seen in the spectra. Simultaneously, there is an appearance of the band at 218 cm$^{-1}$, assigned to the Cu–O stretching [34], which confirms the coordination of the anion to the metal. The correlation and assignments of the bands are listed in Table 4. In Ref. [35], the synthesis of $Cu(ClO_4)_2$ is different from the one used in this work, and there is a high possibility of some impurity being present.

Based on the results summarized in Table 4, in the ex situ SERS spectrum of the Ag/tpy/$ClO_4^-$ system (Fig. 2(c)), the band at 916 cm$^{-1}$ can be assigned to the bidentate $ClO_4^-$ group, and the band at 930 cm$^{-1}$ to the monodentate perchlorates; therefore, both species are adsorbed on the electrode surface. Using the same arguments, the band at 930 cm$^{-1}$ in the in situ SERS spectra of the Ag/tpy/$ClO_4^-$ system (Fig. 3(**II**), at more positive potential, indicates only one kind of perchlorate ion (monodentated) adsorbed on the surface, while, at $-0.7$ V, two bands at 915 and 930 cm$^{-1}$ suggest the presence of bidentate and monodentate perchlorates, respectively, on the surface.

The Raman spectrum of a single crystal of $[Cu^{II}$(t-py)$(H_2O)(ClO_4)_2]$ complex shows a strong band at 930 cm$^{-1}$, indicating only a monodentate perchlorate species (Fig. 7(e)). In the infrared spectrum, the band at 1100 cm$^{-1}$ (Fig. 7(d)) has low relative intensity, indicating the absence of free perchlorate [22]. All these vibrational results are consistent with the X-ray diffraction data, which indicated the presence of two $ClO_4^-$

Table 4
Assignment of fundamental vibrations of perchlorate (in cm$^{-1}$)

| $ClO_4{}^-$ ($T_d$) | | $ClO_4{}^-$ ($C_{3v}$) | | $ClO_4{}^-$ ($C_{2v}$) | |
|---|---|---|---|---|---|
| 932 | $\nu_s(ClO_4)$ ($A_1$) | 940 | $\nu(ClO^*)$ ($A_1$) | 917 | $\nu_s(ClO_2^*)$ ($A_1$) |
| 627 | $\delta_s(ClO)$ ($E$) | 626 | $\rho_r$ ($E$) | 627 | $\delta_s(ClO_2^*)$ ($A_1$) |
| | | | | 645 | $\rho_\tau$ ($A_2$) |
| 1104 | $\nu_{as}(ClO)$ ($F_2$) | 1076 | $\nu_s(ClO_3)$ ($A_1$) | 1014 | $\nu_s(ClO_2)$ ($A_1$) |
| | | 1126 | $\delta_{as}(ClO^*)$ ($E$) | 1042 | $\nu_{as}(ClO_2)$ ($B_1$) |
| | | | | 1149 | $\nu_{as}(ClO_2^*)$ ($B_2$) |
| 460 | $\delta_{as}(ClO)$ ($F_2$) | 435 | $\delta_s(ClO_3)$ ($A_1$) | 417 | $\delta_s(ClO_2)$ ($A_1$) |
| | | 456 | $\delta_{as}ClO_3$ ($E$) | 451 | $\rho_r$ ($B_1$) |
| | | | | 483 | $\rho_r$ ($B_2$) |

*Coordinated oxygen atom.

monocoordinated to the $Cu^{II}$ center, as well as tpy and $H_2O$, resulting in a coordination number six.

The Raman spectrum of polycrystalline $Cu^{II}$–tpy–$ClO_4$ complex, used as a standard compound, changes with the time of laser radiation exposure (Fig. 7(b and c)). As the exposure time increases, the perchlorate band at 457 cm$^{-1}$ gives the bands at 419, 452, 479 cm$^{-1}$, the band at 627 shifts to 623 cm$^{-1}$, and the broad band at 932 cm$^{-1}$ produces those at 906 and 930 cm$^{-1}$. The infrared spectrum shows a strong and broad band at 1100 cm$^{-1}$ assigned to free $ClO_4{}^-$ ion (Fig. 7(a)) [22]. On the other hand, the broad band at 932 cm$^{-1}$ observed in the Raman spectrum (Fig. 7(b)), suggests that both the non-coordinated and monocoordinated perchlorate species are present in the beginning, having practically the same frequency values for this mode (Fig. 6(a and b)). These results suggest a coordination number five for the $Cu^{II}$ ion and the proposed structure is $[Cu^{II}(tpy)(H_2O)(ClO_4)]ClO_4$. One explanation for these spectral changes is that, as the sample exposure time to laser radiation increases, the $H_2O$ molecule dissociates from the metal coordination sphere, and the monodentated $ClO_4{}^-$ ligand simultaneously becomes bidentated (as shown by the three bands near 450 cm$^{-1}$ and the band at 906 cm$^{-1}$), maintaining the coordination number five of the $Cu^{II}$ center. It must be emphasized that, in the case of single crystals during the scanning of the Raman spectrum, $H_2O$ molecules are not released from metal coordination sites under laser radiation, which is consistent with the structure shown in Fig. 1(b), where each $H_2O$ molecule bridges adjacent species by hydrogen bonds.

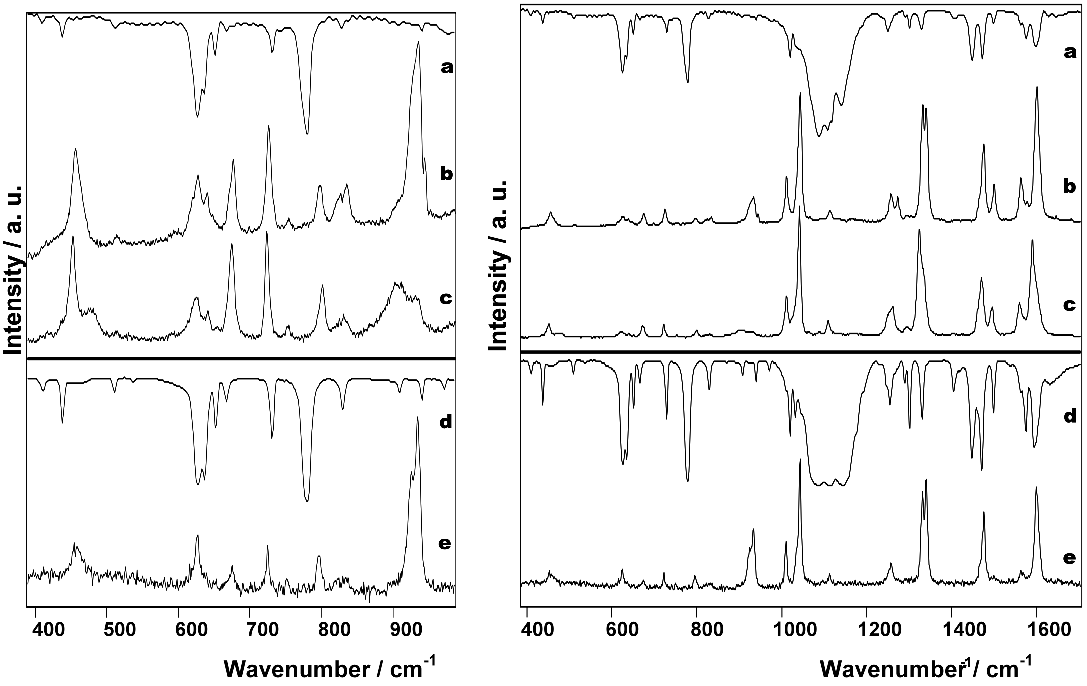

Fig. 7. Vibrational spectra of $[Cu^{II}(tpy)(H_2O)(ClO_4)]ClO_4$ complex: infrared (a), Raman spectra: instantaneous (b) and after 5 min laser exposition (c). Vibrational spectra of single crystal $[Cu^{II}(tpy)(H_2O)(ClO_4)_2]$ complex: infrared (d), Raman (e).

## 4. Conclusions

The different spectral patterns of tpy adsorbed on a metal surface have been rationalized by considering the different interaction of the electron lone pairs of the nitrogen atoms with the surface. The Ag–N bonding in the surface complex type I is similar to the bonding at the Ag–tpy complex, and has higher ionic character because the Ag adatoms in the metallic SERS-active sites have positive average charge. At negative applied potential, these Ag sites have turned to more neutral charge and another surface complex type II has been formed. In this case, the Ag–N bonding is more similar to the Cu–N bonding in the Cu–tpy complexes and possess a higher coordination character.

The tpy–SH SERS studies have confirmed the adsorption through the S atoms, which supports the tpy SERS analysis. The characterization of the $Cu^{II}$ ions on Ag/tpy–SH surfaces has shown that the SERS technique is an excellent tool to monitor the building of molecular devices through the step-by-step deposition of different layers.

It has been possible to identify mono and bidentante $ClO_4^-$ groups, adsorbed on a silver electrode and to characterize the coordination of $ClO_4^-$ in crystals of $Cu^{II}$–tpy complexes, showing that the kind of coordination depends on the recrystallization kinetics.

## 5. Supplementary material

Crystallographic data (excluding structure factors) for the structure(s) reported in this paper have been deposited with the Cambridge Crystallographic Data Centre as supplementary publication number CCDC 196011. Copies of the data can be obtained, free of charge, on application to CCDC, 12 Union Road, Cambridge CB2 1EZ, UK (fax: +44-1223-336033; e-mail: deposit@ccdc.cam.ac.uk or www: http://www.ccdc.cam.ac.uk).

## Acknowledgements

The authors would like to thank the Brazilian Research Agencies, FAPESP and CNPq, for financial support. A.C. Sant'Ana and W.A. Alves are grateful to CNPq and FAPESP for the scholarship grants. M.L.A. Temperini would like to thank Dr H. D. Abruña for furnishing the tpy–SH sample.

## References

[1] J. Baldwin, N. Schühler, I.S. Butler, M.P. Andrews, Langmuir 12 (1996) 6389.

[2] L.A. Dick, A.J. Haes, R.P. Van Duyne, J. Phys. Chem. B 104 (2000) 11752.

[3] I. Srnová-Sloufová, B. Vlcková, T.L. Snoeck, D.J. Stufkens, P. Matejka, Inorg. Chem. 39 (2000) 3551.

[4] M.F. Mrozek, S.A. Wasoleski, M.J. Weaver, J. Am. Chem. Soc. 123 (2001) 12817.

[5] T. Lu, T.M. Cotton, Langmuir 5 (1989) 406.

[6] A.G. Brolo, D.E. Irish, J. Lipkowski, J. Phys. Chem. B 101 (1997) 3906.

[7] Y.S. Pang, H.J. Hwang, M.S. Kim, J. Mol. Struct. 441 (1998) 63.

[8] G. Wang, J. Shi, H. Yang, X. Wu, Z. Zhang, R. Gu, P. Cao, J. Raman Spectrosc. 33 (2002) 125.

[9] M. Kim, K. Itoh, J. Phys. Chem. 91 (1987) 126.

[10] I. Srnová, B. Vlcková, I. Nemec, M. Slouf, J. Stepánek, J. Mol. Struct. 482 (1999) 213.

[11] K. Zawada, J. Bukowska, J. Mol. Struct. 555 (2000) 425.

[12] A.M.W.C. Thompson, Coord. Chem. Rev. 160 (1997) 1.

[13] G. Albano, V. Balzani, E.C. Constable, M. Maestri, D.R. Smith, Inorg. Chim. Acta 277 (1998) 225.

[14] K. Hutchison, J.C. Morris, T.A. Nile, J.L. Walsh, D.W. Thompson, J.D. Petersen, J.R. Schoonover, Inorg. Chem. 38 (1999) 2516.

[15] P. Bonhote, J.E. Moser, R. Humphry-Baker, N. Vlachopoulos, S.M. Zakeeruddin, L. Walder, M. Gratzel, J. Am. Chem. Soc. 121 (1999) 1324.

[16] S. Swavey, Z.L. Fang, K.J. Brewer, Inorg. Chem. 41 (2002) 2598.

[17] S.M. Zakeeruddin, M.K. Nazeeruddin, P. Pechy, F.P. Rotzinger, R. Humphry-Baker, K. Kalyanasundaram, M. Grätzel, Inorg. Chem. 36 (1997) 5937.

[18] L. Cheng, G.E. Pacey, J.A. Cox, Anal. Chem. 73 (2001) 5607.

[19] J.L. Cohen, J. Widera, J.A. Cox, Electroanalysis 14 (2002) 231.

[20] K. Wang, M. Haga, M.D. Hossain, H. Shindo, K. Hasebe, H. Monjushiro, Langmuir 18 (2002) 3528.

[21] M. Maskus, H.D. Abruña, Langmuir 12 (1996) 4455.

[22] B.J. Hathaway, A.E. Underhill, J. Am. Chem. Soc. (1961) 3091.

[23] A.C.T. North, D.C. Phillips, F.S. Mathews, Acta Crystallogr., Sect. A 24 (1968) 359.

[24] L.J. Farrugia, J. Appl. Cryst. 32 (1999) 837.

[25] A. Altomare, G. Cascarano, C. Giacovazzo, A. Guagliardi, J. Appl. Cryst. 26 (1993) 343.

[26] G.M. Sheldrick, SHELX97—programs for crystal structure analysis (Release 97-2). Institüt für Anorganische Chemie der Universität, Tammanstrasse 4, D-3400 Göttingen, Germany, 1998.

[27] A.L. Spek, Acta Crystallogr., Sect. A 46 (1990) C34.

[28] K. Nakamoto, J. Phys. Chem. 64 (1960) 1420.

[29] P.O.'D. Offenhartz, P. George, G.P. Haight, Jr., J. Phys. Chem. 67 (1962) 116.

[30] A. Sarkar, S. Chakravorti, Spectrosc. Lett. 27 (1994) 305.

[31] M.A. Bryant, J.E. Pemberton, J. Am. Chem. Soc. 113 (1991) 3629.

[32] M.A. Bryant, J.E. Pemberton, J. Am. Chem. Soc. 113 (1991) 8284.

[33] C.J. Sandroff, D.R. Herschbach, J. Phys. Chem. 86 (1982) 3277.

[34] S. Kania, R. Holze, Surf. Sci. 408 (1998) 252.

[35] J.L. Pascal, J. Potier, D.J. Jones, J. Rozière, A. Michalowicz, Inorg. Chem. 23 (1984) 2068.